22^{nd} International Conference on Efficiency, Cost, Optimization,
Simulation and Environmental Impact of Energy Systems
August 31 - September 3, 2009, Foz do Iguaçu, Paraná, Brazil

COOLING OF ETHANOL FERMENTATION PROCESS USING ABSORPTION CHILLERS

Felipe Costa Magazoni, magazoni@lepten.ufsc.br
Julieta Barbosa Monteiro, julieta@lepten.ufsc.br
Ricardo Deucher, rdeucher@lepten.ufsc.br
Marcus Vinícius Americano da Costa Filho, mvamericano@lepten.ufsc.br
José Miguel Cardemil, jose.cardemil@lepten.ufsc.br
Sergio Colle, colle@emc.ufsc.br
The Conversion Processes Engineering and Technology Energy Laboratories - LEPTEN
Department of Mechanical Engineering - Federal University of Santa Catarina
88040-900, Florianópolis, Brazil

Abstract. *Ethanol fermentation is an exothermic process, and its kinetics is dependent on temperature. This study proposes an alternative cooling system for use in ethanol fermentation using a single-effect water/lithium bromide absorption chiller, powered by waste heat from sugar and ethanol production, with a temperature range of 80 to* $100\ ^{\circ}\mathrm{C}$*, for example, that of the contaminated condensate from the sugarcane juice evaporation process in sugar production. The aim of this study is to model, simulate and analyze the behavior of a machine for absorption refrigeration, according to the required cooling capacity of the fermentation system. A comparative analysis with and without the chiller is performed. The introduction of a chiller to the cooling system of the vat allowed a reduction in the temperature of the medium of around* $1\ ^{\circ}\mathrm{C}$ *and an increase of around* $0.8\ \%$ *in the fermentation efficiency. The results show that this reduction in temperature can increase the ethanol content of the wine. In the recovery of ethanol, a lower thermal load will be needed in the distillation, a smaller amount of vinasse is produced and consequently the energy efficiency of the plant increases. Under these conditions less cellular stress occurs and cellular viability is kept at higher levels. A thermoeconomic evaluation is performed and shows that the annual cost flow rate difference of the fermentation process increases US$ 75,609.01 per fermentation vat in comparison with the refrigeration system using just the cooling tower, representing a payback period of 1.59 years.*

Keywords. *Absorption chiller, lithium bromide, cooling, fermentation, ethanol, simulation, thermoeconomic analysis*

1 INTRODUCTION

In industrial ethanol fermentation the yeast cells are submitted to stresses inherent to the fermentation process such as ethanol and reducing sugar accumulation and those originating from environmental factors, operating conditions and physico-chemical factors such as high temperature, pH and high salts, ethanol and sugar concentrations. Of these factors, temperature has the greatest effect the fermentation kinetics of the process and cell viability (Phisalaphong et al. 2006). Temperature and ethanol can have synergistic effects on the dynamic behavior of the fermentation process. Another consideration with regard to thermal stress is the formation of by-products such as glycerol and organic acids, mainly succinic and acetic. Studies have shown that the ideal fermentation temperature for increased productivity and maintenance of cell viability is around $32\ ^{\circ}\mathrm{C}$ (Aldiguier et al. 2004; Phisalaphong et al. 2006).

Currently, the Brazilian ethanol and sugar plants use cooling towers to chill the fermentation process, but these fail to reduce and maintain the temperature of the fermentation medium, since they are dependent on the inclimate of the region, and this is detrimental to the good performance of the equipment. A small deviation in temperature can affect the kinetic behavior of the fermentation as well as the degree of contamination by bacteria and the development of new *S. cerevisiae* strains, as well as wild yeast, and non-*Saccharomyces* species (Torija et al. 2003). There is also a correlation between the ethanol tolerance of yeast cells and fermentation temperature (Aldiguier et al. 2004). The temperature also affects the osmotolerance of yeast cells. This factor should be considered especially when cane molasses is used as the substrate. Thus, a cooling system capable of removing the heat released in order to reduce and keep the fermentation temperature at ideal values is required.

An absorption chiller is thermally driven cooling equipment, which requires little external work. These machines become economically attractive when there is a residual thermal energy source available, such as geothermal energy, solar energy and waste heat from thermal processes (hot exhaust gas discharges, hot water discharges and waste low pressure steam). Single-effect absorption technology provides a peak cooling coefficient of performance of approximately 0.8 and operates with heat input temperatures in the range of 75 to $100\ ^{\circ}\mathrm{C}$ (Herold et al. 1996). This study proposes an alternative cooling system for use in ethanol fermentation using a single-effect water/lithium bromide absorption chiller, powered by waste heat from sugar and alcohol production, for example, the contaminated condensate ($96\ ^{\circ}\mathrm{C}$) from the sugarcane juice evaporation process during sugar production, vinasse ($80\ ^{\circ}\mathrm{C}$) and flash saturated steam ($100\ ^{\circ}\mathrm{C}$).

Nomenclature

a	activity
c	cost per exergy unit, US\$ GJ^{-1}
$\dot{C}$	cost flow rate, US\$ h^{-1}
COP	coefficient of performance
Cp	specific heat capacity, kJ kg^{-1} K^{-1}
e	specific exergy, kJ kg^{-1}
E	ethanol concentration, kg m^{-3}
$\dot{E}$	exergy flow rate, kW
$\dot{F}$	substrate feed volume flow rate, m^3 h^{-1}
h	enthalpy, kJ kg^{-1}
K_i	substrate inhibition coefficient, m^3 kg^{-1}
K_S	substrate saturation constant, kg m^{-3}
M	molecular mass, kg kmol^{-1}
$\dot{m}$	mass flow rate, kg h^{-1}
m_E	ethanol production associated with growth, kg kg^{-1} h^{-1}
m_X	maintenance coefficient, kg kg^{-1} h^{-1}
n	product inhibition power
P	pressure, kPa
pr	productivity, kg m^{-3} h^{-1}
$\dot{Q}$	heat flow, kW
$\widetilde{R}$	universal gas constant, kJ kmol^{-1} K^{-1}
s	specific entropy, kJ kg^{-1} K^{-1}
S	substrate concentration, kg m^{-3}
t	time, h
T	temperature, °C
UA	overall thermal conductance, kW K^{-1}
V	working volume, m^3
$\dot{V}$	volume flow rate, m^3 h^{-1}
X	cell concentration, kg m^{-3}
y	mole fraction
Y	yield factor, kg kg^{-1} or exergy destruction ratio
$\dot{W}$	power, kW
$\dot{Z}$	levelized investment cost, US\$ h^{-1}

Greek symbols

ΔH_S	fermentation heat released, kJ kg^{-1}
Δt	time difference, h
$\widetilde{\varepsilon}$	standard chemical exergy, kJ mol^{-1}
η	efficiency, %
μ	specific growth rate, h^{-1}
ρ	density, kg m^{-3}
ξ	lithium bromide mass fraction, %

Subscripts

0	initial time or reference state
1–23	status point in Fig. 1
a	absorber
ch	chemical
c	condenser
$cryst$	crystallization
D	destruction
Δt	time difference
e	evaporator
E	ethanol
f	fermentation
F	fuel
fhx	fermentation heat exchanger
g	generator
H	hot side
hx	heat exchanger
in	inlet
$LiBr$	lithium bromide
max	maximum
out	outlet
p	pump
P	product
ph	physical
sol	solution
S	substrate
t	time
X	cell
w	water

The thermoeconomic evaluation of a lithium bromide absorption refrigeration is carried out to calculate the thermoeconomic parameters, based on the Specific Exergy Costing, discussed by Lazzaretto and Tsatsaronis (2006) and Misra et al. (2003).

The aim of this study is to investigate the behavior of the fermentation process with the introduction of an absorption chiller in the cooling system of the fermentation vats, currently in use in an industrial ethanol fermentation process (Usina Cerradinho Açúcar e Álcool S/A).

2 MATERIALS AND METHODS

2.1 System description

A schematic diagram of the cooling system for ethanol fermentation is shown in Fig. 1. This figure represents the fermentation module of the ethanol industrial process and it consists of the components: single-effect absorption chiller and fermentation system.

The components of the single-effect water/lithium bromide absorption chiller, shown in region I of Fig. 1, are: generator, absorber, condenser, evaporator, solution heat exchanger, solution pump, expansion valve and throttling valve. Firstly, the weak solution of lithium bromide is pumped from the low pressure in the absorber to the high pressure in the generator

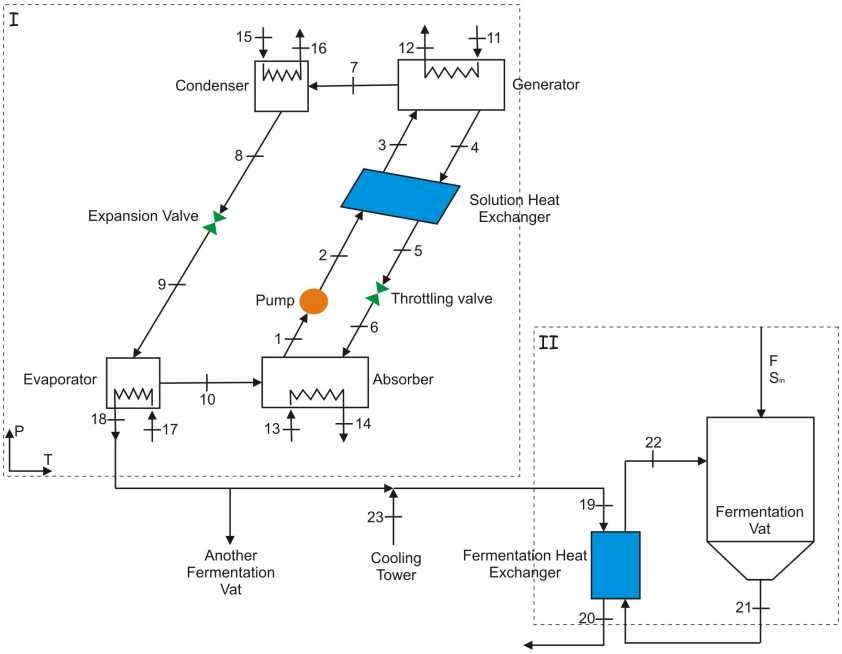

Figure 1: Schematic diagram of the cooling system for ethanol fermentation using a single-effect absorption chiller

where heat is supplied by the waste heat source (point 11) and the refrigerant water is separated from aqueous lithium bromide solution by evaporation. The superheated steam (point 7) goes through the condenser where it is condensed on the surface of a cooling coil. The saturated water that leaves the condenser is throttled through the expansion valve to the lower pressure in the evaporator, where it evaporates by absorbing heat and provides cooling capacity (point 18). The saturated steam from the evaporator (point 10) flows to the absorber where it is absorbed by the strong solution from the generator. The mixing process in the absorber is exothermic and needs to reject heat to the water from the condenser. The weak solution, which leaves the absorber, is pumped to the generator and goes through the solution heat exchanger where it is cooled, and the refrigeration process begins again.

One constraint of the single-effect water/lithium bromide absorption chiller is the crystallization of the absorbent (lithium bromide) and the point of the cycle most vulnerable in this regard is the stream entering the absorber (point 6), because of its high concentrated solution and low temperature.

The absorption chiller has a nominal cooling capacity of 3000 kW and it chills two fermentation vats. The cooling capacity of the absorption chiller was selected considering the availability of waste heat at the plant. This study only shows the refrigeration of one fermentation vat, thus the mass flow rate of the chilled water from the evaporator is divided into two streams. The volume flow rate, the temperature and the cost per exergy unit of some streams in the absorption chiller are shown in Tab. 1. The configuration of the water loop inlet in the absorption chiller is: condenser (point 15) and evaporator (point 17) use the water from the cooling tower, the absorber uses the water that leaves the condenser (point 16) to reject heat and the generator is heated by the contaminated condensate from the broth evaporation process during sugar production (point 11). The water from the cooling tower T_{23} is used to refrigerate the fermentation vat and the absorption chiller. The heat source is assumed to be free ($c_{11} = 0$) and the value of the cost per exergy unit of the point 15 is estimated using the water price (5 US\$ m^{-3}). The simulation of the cooling tower is out of analysis.

Table 1: Volume flow rate, temperature and cost per exergy unit of some streams in the absorption chiller

Point	$\dot{V}$ ($\mathrm{m}^3\,\mathrm{h}^{-1}$)	T (°C)	c (US\$ GJ^{-1})
1	26	–	–
11	350	96	0
13	800	T_{16}	c_{16}
15	800	T_{23}	100
17	450	T_{23}	c_{15}

The ethanol fermentation (region II in Fig. 1) is a biochemical process where the sugars are transformed into alcohol by industrial yeast *Saccharomyces cerevisiae*. The carbon source used is cane molasses. The fermentation time ranges from 4 to 6 h plus the wait time (1 to 3 h) and there are two fermentation processes per day and two hundred and forty days per year of industrial processing for each vat. At the end of the fermentation, all sugars have been consumed and the

final fermentation product, called wine, has an ethanol concentration of 60 to 90 $\mathrm{kg\,m^{-3}}$.

The heat released during the ethanol fermentation is removed by means of a plate heat exchanger, where the cold stream (point 19) is provided by both streams, water from the cooling tower (point 23) and from the evaporator of the absorption chiller (point 18). The must from the fermentation vat (point 21) flows to the fermentation heat exchanger with a constant volume flow rate and the flow rate of the cold stream (point 19) is used as a manipulated variable to control the fermentation temperature.

The heat exchangers of the process are in a counter flow arrangement. Plate heat exchangers are used at the solution heat exchanger of the absorption chiller and fermentation heat exchanger, while those of the absorption chiller are shell and tube heat exchangers. The absorption chiller's heat exchangers are made of copper while the fermentation heat exchanger is made of stainless steel AISI 304. The overall thermal conductances UA of heat exchangers and the levelized investment cost associated with system components are shown in Tab. 2. The thermoeconomic parameters and the levelized investment cost $\dot{Z}$ are calculated using the following assumptions:

- The capital cost of absorption chiller is 160 $\mathrm{US\$\,kW^{-1}}$ (37.99 % is of the absorber, 26.23 % of the generator, 9.50 % of the condenser, 20.09 % of the evaporator, 5.31 % of the solution heat exchanger and 0.88 % of the solution pump), as described in Bereche (2007);
- Installation of the absorption unit: 25 % of the total capital cost;
- Electric energy price: 50 $\mathrm{US\$\,MW^{-1}\,h^{-1}}$;
- Ethanol price: 400 $\mathrm{US\$\,m^{-3}}$;
- Discount rate: 15 % per year;
- Operational time: 5,760 h per year;
- Analysis period: ten years.

Table 2: Overall heat transfer coefficients of heat exchangers and levelized investment cost for each component of the system

Component	UA ($\mathrm{kW\,K^{-1}}$)	$\dot{Z}$ ($\mathrm{US\$\,h^{-1}}$)
Generator	165.0	5.16
Absorber	297.0	7.48
Condenser	198.0	1.88
Evaporator	371.3	3.16
Solution heat exchanger	31.6	1.05
Fermentation heat exchanger	966.4	6.17
Solution pump	–	0.18

2.2 Mathematical modeling

2.2.1 Absorption chiller

The modeling of the absorption chiller is performed based on energy, mass and species balances, considering a quasi-steady state regime (the system moves quickly through a sequence of steady states, even while subjected to varying conditions over time), according to the theoretical fundamentals of Herold et al. (1996).

The mass flow rate balance of the generator is calculated as

$$\dot{m}_3 = \dot{m}_4 + \dot{m}_7 \tag{1}$$

Considering that there is no lithium bromide in the superheated steam (point 7), the lithium bromide balance in the generator is given by the equation below

$$\dot{m}_3 \cdot \xi_3 = \dot{m}_4 \cdot \xi_4 \tag{2}$$

where ξ_3 is the lithium bromide mass fraction of the weak solution and ξ_4 is the lithium bromide mass fraction of the strong solution.

The solution pump reaches the steady state flow rate quickly and maintains a constant rate. The expression of the work input of the solution pump is obtained as

$$\dot{W}_p = 100 \cdot \left[\frac{\dot{m}_1 \cdot (P_2 - P_1)}{\eta_p \cdot \rho_1} \right] \tag{3}$$

where η_p is the solution pump efficiency and its value is 72 % and ρ_1 is the density of the aqueous lithium bromide solution at point 1 in Fig. 1.

The modeling of the heat exchanger-cycle cooling system of the absorption chiller is carried out using the energy balance and the Logarithmic Mean Temperature Difference (LMTD) as described in Bejan and Kraus (2003).

The coefficient of performance COP of the absorption chiller is defined as follows

$$COP = \frac{\dot{Q}_e}{\dot{Q}_g + \dot{W}_p} \tag{4}$$

where $\dot{Q}_e$ is the cooling capacity, $\dot{Q}_g$ is the heat flow input in the generator and $\dot{W}_p$ is the work input of the solution pump.

2.2.2 Fermentation

The mathematical model for the ethanol fermentation is an unstructured model and the modeling is performed based on kinetic rate models coupled with mass balance equations for the cell, substrate and ethanol and the energy balance, for an industrial fed-batch fermentation process. It is assumed that the feed is sterile ($X_{in} = 0$).

The global mass balance is described as

$$\frac{dV}{dt} = \dot{F} \tag{5}$$

where $\dot{F}$ is the substrate feed volume flow rate and dV/dt represents the variation in the working volume during the fermentation process.

The rate of cell growth is defined as follows

$$\frac{dX}{dt} = \mu \cdot X - \frac{\dot{F} \cdot X}{V} \tag{6}$$

where μ is the specific growth rate and the factor $\dot{F}/V$ is the dilution rate as the feed is added during the fermentation process.

The substrate consumption is modeled by the following equation

$$\frac{dS}{dt} = -\frac{\mu \cdot X}{Y_{X/S}} - m_X \cdot X + \frac{\dot{F}}{V} \cdot (S_{in} - S) \tag{7}$$

where $Y_{X/S}$ is the yield factor of the cell based on the substrate consumption and m_X is the maintenance coefficient.

The ethanol formation is written as

$$\frac{dE}{dt} = \frac{Y_{E/S} \cdot \mu \cdot X}{Y_{X/S}} + m_E \cdot X - \frac{\dot{F} \cdot E}{V} \tag{8}$$

where $Y_{E/S}$ represents the yield factor of ethanol based on substrate consumption and m_E is the ethanol production associated with growth.

The variation in fermentation temperature T_{21} during the process is described by Eq. (9) and it is determined through the energy balance of the fermentation system.

$$\frac{dT_{21}}{dt} = \frac{\dot{F}}{V} \cdot (T_{in} - T_{21}) - \frac{\dot{V}_{21}}{V} \cdot (T_{21} - T_{22}) + \left(\frac{\Delta H_S}{\rho_{in} \cdot Cp_{in}}\right) \cdot \left(\frac{\mu \cdot X}{Y_{X/S}} + m_X \cdot X\right) \tag{9}$$

where ΔH_S is the heat released during the fermentation process and its value is 697.7 kJ per kilogram of substrate consumed (Albers et al. 2002), the inlet temperature T_{in} and the volume flow rate $\dot{V}_{21}$ are shown in Tab. 6.

In the model shown, the specific growth rate μ is expressed as a function of limiting substrate concentration S (Monod equation) and of the inhibitory effects of substrate and ethanol concentration (Ghose and Tyagi 1979), as represented by the following equation

$$\mu = \mu_{max} \cdot \left(\frac{S}{K_S + S}\right) \cdot \exp\left(-K_i \cdot S\right) \cdot \left(1 - \frac{E}{E_{max}}\right)^n \tag{10}$$

where μ_{max} is the maximum specific growth rate, K_S is the substrate saturation constant, K_i is the substrate inhibition coefficient, E_{max} is the maximum of ethanol concentration at which yeast cell growth is completely inhibited and n is the product inhibition power. Cell inhibition and death are not taken into account in the model due to the dilution effect in the fed-batch mode and the short residence time. This inhibition occurs at high yeast cell concentration, with cell recycle

(Jarzebski and Malinowski 1989; Lee et al. 1983). Under industrial conditions, the microorganism is a yeast isolated from the industrial environment and therefore adapted to fermentation stress. In addition, in each fermentation cycle the yeast receives an acid treatment for 2 to 3 h, when nutrients are also supplied.

The parameters used in the model shown above were taken from literature Atala et al. (2001) and are presented in Tab. 3. These expressions were determined for the temperature ranging from 28 to 40 °C, using an industrial yeast *Saccharomyces cerevisiae* and cane molasses as substrate.

Table 3: Kinetic parameters as a function of temperature

Parameter	Expression or Value
μ_{max}	$1.57 \cdot \exp\left(-\frac{41.47}{T_{21}}\right) - 1.29 \cdot 10^4 \cdot \exp\left(-\frac{431.4}{T_{21}}\right)$
E_{max}	$-0.4421 \cdot T_{21}^2 + 26.41 \cdot T_{21} - 279.75$
$Y_{X/S}$	$2.704 \cdot \exp\left(-0.1225 \cdot T_{21}\right)$
$Y_{E/S}$	$0.6911 \cdot \exp\left(-0.0139 \cdot T_{21}\right)$
K_i	$1.393 \cdot 10^{-4} \cdot \exp\left(0.1004 \cdot T_{21}\right)$
K_S	4.1
m_E	0.1
m_X	0.2
n	1.5

The heat flow rate released during the fermentation process $\dot{Q}_f$ is calculated as follows

$$\dot{Q}_f = \Delta H_S \cdot \left[\frac{V_{t-\Delta t} \cdot (S_{t-\Delta t} + S_{in}) - V \cdot S}{3600 \cdot \Delta t}\right] \tag{11}$$

where $S_{t-\Delta t}$ and $V_{t-\Delta t}$ represent the substrate concentration and the working volume of the fermentation vat at past time, S and V is the substrate concentration and the working volume at the present time and Δt represents the time difference.

The fermentation heat exchanger is modeled using the Logarithm Mean Temperature Difference (LMTD) method and the energy balance as described in Bejan and Kraus (2003).

The fermentation efficiency may be written as

$$\eta_f = 100 \cdot \left\{\frac{E \cdot V - E_0 \cdot V_0}{0.511 \cdot [V \cdot (S_{in} - S) - V_0 \cdot (S_{in} - S_0)]}\right\} \tag{12}$$

where 0.511 is the sugar to ethanol conversion factor based on the theoretical maximum yield.

The ethanol productivity is calculated by the following expression

$$pr_E = \frac{E \cdot V - E_0 \cdot V_0}{V \cdot t} \tag{13}$$

2.2.3 Thermoeconomic analysis

Thermoeconomic evaluation is a method to determine the actual cost of products or services or to provide information on which operating decisions may be based and evaluated (Bejan et al. 1996). Thus, the thermoeconomic analysis requires an exergy analysis for the absorption system and consists in the calculation of physical and chemical exergy of aqueous lithium bromide solution, following exergy cost.

The total specific exergy is divided into two main components: specific physical exergy e_{ph} and specific chemical exergy e_{ch}, and it can be described as

$$e = e_{ph} + e_{ch} \tag{14}$$

The specific physical exergy at a specified state is given by the expression

$$e_{ph} = (h - h_0) - T_0 \cdot (s - s_0) \tag{15}$$

where h_0, s_0 and T_0 denote, respectively, the specific enthalpy, specific entropy and temperature in Kelvin at the reference state ($T_0 = 298.15$ K and $P_0 = 101.325$ kPa).

The specific chemical exergy of the aqueous lithium bromide solution can be calculated trough the expression proposed

by Bejan et al. (1996) and Bereche (2007),

$$e_{ch} = \frac{1}{M_{sol}} \cdot \left\{ (y_w \cdot \widetilde{\varepsilon}_w + y_{LiBr} \cdot \widetilde{\varepsilon}_{LiBr}) + \widetilde{R} \cdot T_0 \cdot \left[y_w \cdot \ln(a_w) + y_{LiBr} \cdot \ln(a_{LiBr}) \right] \right\} \tag{16}$$

where M_{sol} is the molecular mass of the aqueous lithium bromide solution, y_w and y_{LiBr} denote, respectively, the mole fraction of water and lithium bromide at the solution, $\widetilde{\varepsilon}$ is the standard chemical exergy of water (0.9 kJ mol^{-1}) and lithium bromide (101.6 kJ mol^{-1}) taken in Szargut et al. (1988), a_w and a_{LiBr} are respectively the activity of the water and lithium bromide (Bereche 2007), and $\widetilde{R}$ is the universal gas constant (8.314 kJ kmol^{-1} K^{-1}).

The exergy destruction $\dot{E}_d$, the amount of exergy that is lost to the environment and cannot be used anywhere, is calculated from the exergy balance as

$$\dot{E}_D = \sum \dot{E}_{in} - \sum \dot{E}_{out} - \dot{W} - \dot{Q} \cdot \left(1 - \frac{T_0}{T}\right) = \dot{E}_F - \dot{E}_P \tag{17}$$

where $\dot{E}_F$ and $\dot{E}_P$ are the exergy flow rate associated to the fuel and the exergy flow rate associated to the product, respectively (Tab. 4), and $\dot{E}$ is the exergy flow rate ($\dot{E} = \dot{m} \cdot e$).

Table 4: Exergy flow rate associated with the fuel and product in the absorption system

Component	$\dot{E}_F$	$\dot{E}_P$
Generator	$\dot{E}_{11} - \dot{E}_{12}$	$\dot{E}_4 + \dot{E}_7 - \dot{E}_3$
Absorber	$\dot{E}_6 + \dot{E}_{10} - \dot{E}_1$	$\dot{E}_{14} - \dot{E}_{13}$
Condenser	$\dot{E}_8 - \dot{E}_7$	$\dot{E}_{15} - \dot{E}_{16}$
Evaporator	$\dot{E}_9 - \dot{E}_{10}$	$\dot{E}_{18} - \dot{E}_{17}$
Solution heat exchanger	$\dot{E}_4 - \dot{E}_5$	$\dot{E}_3 - \dot{E}_2$
Fermentation heat exchanger	$\dot{E}_{22} - \dot{E}_{21}$	$\dot{E}_{19} - \dot{E}_{20}$
Solution pump	$\dot{W}_p$	$\dot{E}_2 - \dot{E}_1$
Overall system	$\dot{E}_{11} - \dot{E}_{12}$	$\dot{E}_{18} - \dot{E}_{17}$

The exergy destruction ratio Y_D of the components is the ratio of exergy destruction by the total exergy supplied to the system,

$$Y_D = \frac{\dot{E}_D}{\dot{E}_{F,system}} \tag{18}$$

where $\dot{E}_{F,system}$ is the exergy flow rate associated to the fuel for absorption system.

The cost balance equation for a component receiving a heat transfer and generating power is

$$\sum \left(\dot{E} \cdot c\right)_{out} + \dot{C}_W = \sum \left(\dot{E} \cdot c\right)_{in} + \dot{C}_Q + \dot{Z} \tag{19}$$

where c is the cost per exergy unit, $\dot{C}$ is the cost flow rate and $\dot{Z}$ is the levelized investment cost associated with system components shown in Tab. 2. The auxiliary equations for the determination of the cost per exergy unit are given in Tab. 5.

Table 5: Auxiliary equations for the determination of the cost per exergy unit

Component	**Auxiliary Equation**
Generator	$\dfrac{\dot{C}_4 + \dot{C}_7}{\dot{E}_4 + \dot{E}_7} = \dfrac{\dot{C}_3}{\dot{E}_3}$
Absorber	$\dfrac{\dot{C}_6 + \dot{C}_{10}}{\dot{E}_6 + \dot{E}_{10}} = \dfrac{\dot{C}_1}{\dot{E}_1}$
Condenser	$c_8 = c_7$
Evaporator	$c_{10} = c_9$
Solution heat exchanger	$c_5 = c_4$
Fermentation heat exchanger	$c_{20} = c_{19}$
Throttling valve	$c_6 = c_5$
Expansion valve	$c_9 = c_8$

Thus, the cost flow rate difference of the fermentation vat and fermentation heat exchanger $\Delta\dot{C}_f$ can be calculated by

the following expression

$$\Delta\dot{C}_f = \dot{C}_{19} - \dot{C}_{20} + \dot{Z}_{fhx} + \dot{Z}_f \tag{20}$$

where $\dot{Z}_{fhx}$ is the levelized investment cost for the fermentation heat exchanger and $\dot{Z}_f$ is the levelized investment cost for the fermentation process, that can be calculated using the ethanol production in the fermentation vat. The value of the cost flow rate difference $\Delta\dot{C}_f$ can represent an income (negative) or an expensive (positive). For the fermentation process, the value of the cost flow rate difference is negative, because there is production of ethanol during the fermentation process.

2.3 Simulation

The data collected at Usina Cerradinho Açúcar e Álcool S/A are shown in Tab. 6 and they are used as the initial conditions for the simulation of the industrial fermentation process. For the fermentation, the feed flow rate of the must $\dot{F}$ and the inlet must temperature T_{in} change according to the expressions given in the table. The values for the feed substrate concentration S_{in}, initial cell X_0 and ethanol E_0 concentrations, initial temperature T_0 and initial volume V_0 are shown. The initial time of the refrigeration process is 0.45 h. The water temperature of the cooling tower T_{23} and volume flow rate $\dot{V}_{19}$ were taken during the fermentation process under industrial conditions at Usina Cerradinho Açúcar e Álcool S/A and the temperatures vary according to the expression shown.

Table 6: Fermentation data collected at Usina Cerradinho Açúcar e Álcool S/A

Parameter	Expression or Value
$\dot{F}$	$8.73 \cdot t + 76.29$
S_{in}	200
E_0	34.56
X_0	71.6
T_0	28.37
T_{in}	$0.15 \cdot t + 31.43$
T_{23}	$-0.05 \cdot t^2 + 0.78 \cdot t + 26.03$
V_0	210
$\dot{V}_{19}$	$-60.0 \cdot t + 1030.1$
$\dot{V}_{21}$	1000

The simulations were performed using the program Engineering Equation Solver (EES®) developed by Klein and Alvarado (2008). The properties of the water were evaluated with the correlations given by IAPWS (1995). The specific enthalpy of the aqueous lithium bromide solution was calculated in terms of the solution temperature and lithium bromide mass fraction using the correlation given by ASHRAE (2001). The density of the aqueous lithium bromide solution is given by the equation of Patterson and Perez-Blanco (1988). The correlations of the heat capacity and density of the sugarcane juice used in this work were calculated by Rao et al. (2009).

3 RESULTS AND DISCUSSION

The cell X, substrate S and ethanol E concentration profiles and the fermentation temperature T_{21} during the fermentation process, using only the cooling tower to chill the vat, are shown in Fig. 2. The final concentration of ethanol in the simulated fermentation reaches $73.60\ \mathrm{kg\,m^{-3}}$ against a value of $73.41\ \mathrm{kg\,m^{-3}}$ obtained in the industrial fermentation under analysis, representing a difference of $0.3\ \%$, and an ethanol fermentation effciency of $88.4\ \%$. Considering 8 h of process (fermentation time plus wait time), the ethanol productivity is $7.9\ \mathrm{kg\,m^{-3}\,h^{-1}}$. As seen from the figure, the fermentation temperature reaches a maximum of around 36 °C. Considering that the ideal temperature for the fermentation process is around 32 °C, the use of water from the cooling tower as the only refrigeration source leads to a lower efficiency of the fermentation process.

For the absorption chiller and cooling tower configuration, the mass flow rate of the absorption chiller (point 18) is used to chill two fermentation vats and only half of the mass flow rate from the cooling tower is used, because some of this stream is used in the absorption chiller. As seen from the Fig. 3, the fermentation temperature decreases by around 1 °C with the absorption chiller/cooling tower and the final ethanol concentration is $74.17\ \mathrm{kg\,m^{-3}}$, increasing the ethanol concentration by about $0.57\ \mathrm{kg\,m^{-3}}$, which represents an annual ethanol increase of around $240\ \mathrm{m^3}$ per fermentation vat. The fermentation efficiency is $89.2\ \%$ and ethanol productivity is $8.0\ \mathrm{kg\,m^{-3}\,h^{-1}}$, considering 8 h of fermentation.

With the cooling system shown in Fig. 1, the cooling capacity of the chiller is not sufficient to remove all the heat released during the fermentation. The fermentation temperature T_{21} continues to vary and differs greatly from the ideal temperature (32 °C). A simulation with the fermentation temperature kept constant at 32 °C during the whole process was performed, and the final ethanol concentration reached $75.37\ \mathrm{kg\,m^{-3}}$, representing an annual ethanol increase of

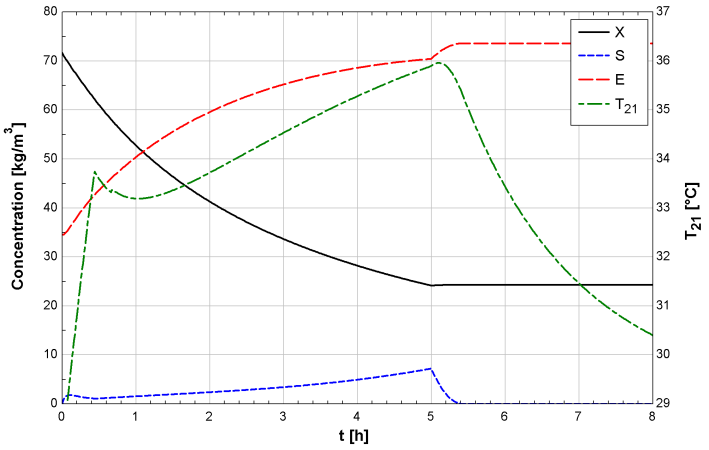

Figure 2: Ethanol E, substrate S and cell X concentration profiles for a fed-batch ethanol fermentation process using the cooling tower to chill the vat

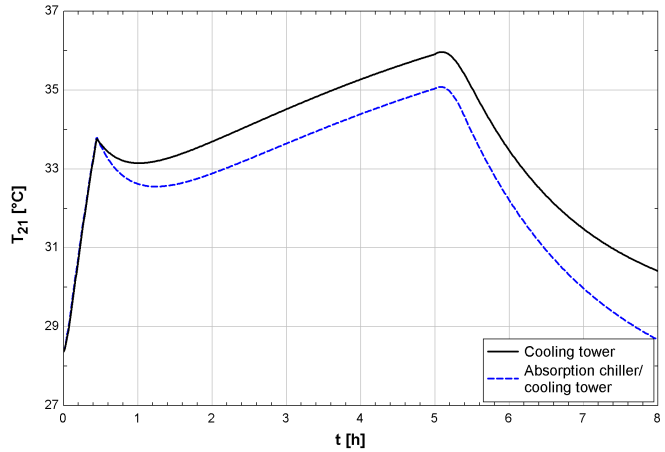

Figure 3: Fermentation temperature profiles T_{21} using the cooling tower and the absorption chiller/cooling tower

around 770 m^3 per fermentation vat. In this case, the fermentation efficiency and the ethanol productivity are 90.9 % and 8.1 $\mathrm{kg\ m^{-3}\ h^{-1}}$, respectively. The fermentation efficiency increased 2.5 % in comparison with that of the refrigeration system with only the cooling tower.

Thus, keeping the fermentation temperature at the ideal value can readily give several improvements in the process such as fermentation efficiency, productivity and cell viability. At high temperatures, the specific growth rate of contaminant microorganisms is increased, however increasing the degree of contamination in the process. The contamination causes flocculation of the yeast cells, leading to problems in the centrifugation besides the high cost of the antibiotic. The high ethanol concentration combined with the high temperatures submits the cells to stress conditions. Under these conditions the yeast has a higher tendency to produce glycerol, which is the main by-product of ethanol fermentation. Thus, lower temperatures reduce the glycerol production, increasing the process efficiency.

Working with a lower fermentation temperature, the inlet substrate concentration S_{in} of the vat can increase and does not adversely affect the fermentation process. Thus, increasing the inlet substrate concentration, the production of ethanol in the fermentation vat increases and the wine with higher ethanol concentration goes to the distillery, producing a smaller amount of vinasse and using a lower thermal load (Camargo et al. 1990). The optimization of the fermentation process to increase the ethanol productivity, maintain cell viability and decrease the fermentation time, is needed when a higher inlet substrate concentration is used.

The heat flow released during the fermentation $\dot{Q}_f$ and the heat flow of the fermentation heat exchanger $\dot{Q}_{fhx}$ with the absorption chiller/cooling tower are shown in Fig. 4. As seen from the figure, the heat flow of fermentation is greater than the heat flow of the heat exchanger, thus the fermentation temperature increases during the process. The ideal process would be when the heat flow released and the heat flow of heat exchanger are the same. This can be achieved by controlling the fermentation temperature using the chilled water flow valve as the manipulated variable or using cold water with a high mass flow rate to maintain the ideal temperature.

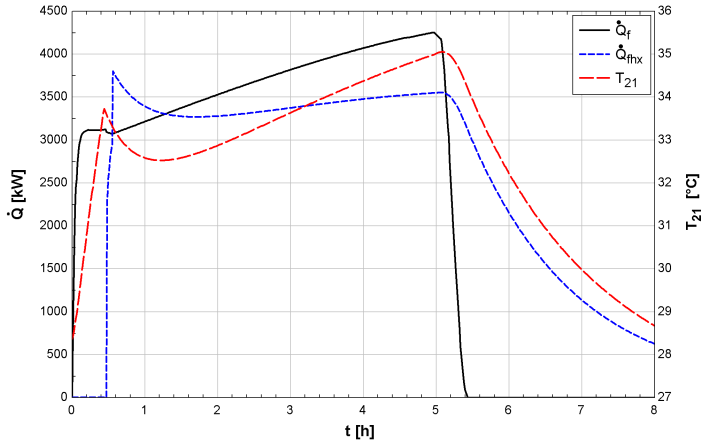

Figure 4: Heat flow rate released during the ethanol fermentation $\dot{Q}_f$, heat flow rate of the fermentation heat exchanger $\dot{Q}_{fhx}$ and fermentation temperature T_{21}

The profiles of some parameters of the absorption chiller during the fermentation process can be observed in Fig. 5. The lithium bromide concentrations of the weak solution ξ_3 and the strong solution ξ_4 are shown in Fig. 5(a). The concentrations and the concentration difference $\Delta\xi$ between the strong and the weak solution decrease during the ethanol fermentation. Thus the mass flow rate of superheated steam (point 7) decreases, and the cooling capacity $\dot{Q}_e$ of the absorption chiller also decreases, as seen in Fig. 5(b). The crystallization line ξ_{cryst} presented in Fig. 5(a) shows the value of the lithium bromide mass fraction at point 6 from which the crystallization process occurs. The difference between the lithium bromide mass fraction of the strong solution ξ_4 and the mass fraction of the crystallization point ξ_{cryst} is around 10 %, showing that the operational conditions of the absorption chiller differ considerably from those of the crystallization phenomenon.

Similarly, the profile of the heat flow input in the absorption chiller was obtained during the fermentation process and is shown in Fig. 5(b). The cooling capacity $\dot{Q}_e$ decreases by around 4 % during the process. Thus it can affect the fermentation temperature and reduce the fermentation efficiency. There are some alternatives available to increase the cooling capacity of the machine such as: increasing the water loop inlet temperature generator T_{11} or decrease the water temperature from the cooling tower T_{23} that enters in the condenser T_{15} and evaporator T_{17}. The effect on the coefficient of performance is negligible and the overall COP value of is 0.81.

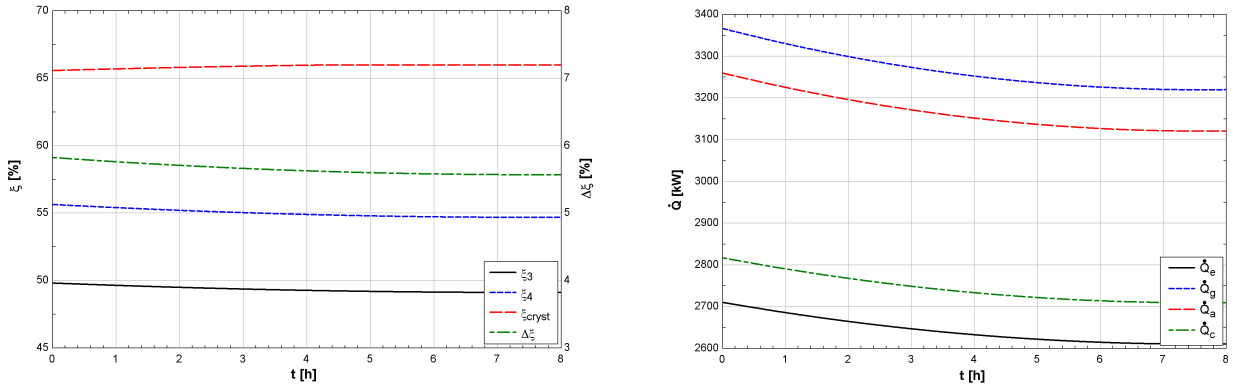

(a) Variation of the lithium bromide mass fraction of absorption chiller

(b) Heat flow input in the evaporator, generator, absorber and condenser

Figure 5: Parameters of absorption chiller during the fermentation process

During the fermentation process, the water loop outlet evaporator temperature T_{18} increases by around 3 °C, because of the temperature variation of the water from the cooling tower. The water loop outlet generator temperature T_{12} is around 88 °C. This stream can still be used in another process to improve the energy efficiency of the plant, either in a cooling capacity or to improve other processes such as air conditioning systems, sugar dryers, recovery of alcoholic gas in the distillery and cooling of must or wine.

The water temperature from the cooling tower T_{23} is an important parameter which affects the performance and the cooling capacity of the absorption chiller. As seen in Fig. 6, on increasing the water temperature, the heat flow input in

the absorption chiller decreases. The cooling capacity $\dot{Q}_e$ is sensitive to the cooling tower and it is essential to keep the water temperature as low as possible. For each $1\ ^{\circ}\mathrm{C}$ increase in the water temperature from the cooling tower, the cooling capacity of the absorption chiller decreases by around $35\ \mathrm{kW}$, this is the cause of the reduction in the cooling capacity shown in Fig. 5(b).

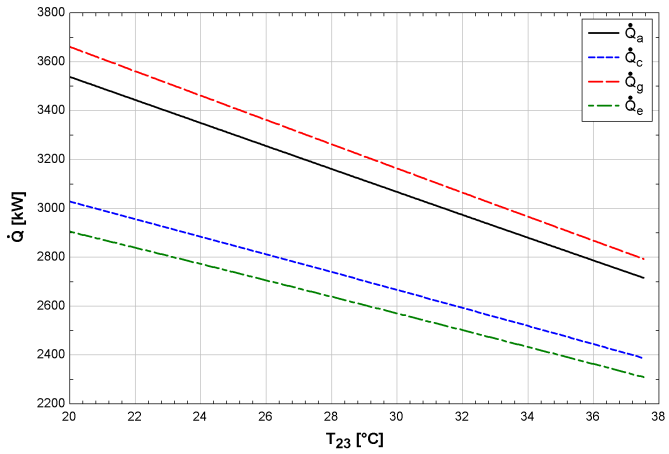

Figure 6: Heat flow input in the absorption chiller with the variation in the temperature of the water from cooling tower

The overall exergy destruction for each component of the system can be observed in Tab. 7. The results show that the maximum exergy destruction ratio is at the generator with $38.8\ \%$, followed by absorber with $25.1\ \%$. Thus, these components can be improved in order to decrease the exergy destruction and increase the system performance.

Table 7: Overall exergy flow rate and exergy destruction ratio of the system components

Component	$\dot{E}_D$ (kW)	$\dot{E}_P$ (kW)	$\dot{E}_F$ (kW)	Y_D (%)
Generator	232.81	367.11	599.92	38.8
Absorber	150.44	79.88	230.32	25.1
Condenser	120.29	41.04	161.33	20.0
Evaporator	54.52	8.30	62.82	9.1
Solution heat exchanger	12.12	11.32	23.44	2.0
Solution pump	0.07	0.00	0.07	0.0

With the refrigeration using just the cooling tower to refrigerate the fermentation vat, the overall cost flow rate difference of the fermentation vat and fermentation heat exchanger $\Delta\dot{C}_f$ is $-2{,}841.38\ \mathrm{US\$\,h^{-1}}$ and the cost per exergy unit difference is $-132.16\ \mathrm{US\$\,MW^{-1}\,h^{-1}}$. With the absorption chiller and cooling tower configuration, the overall cost flow rate difference $\Delta\dot{C}_f$ is $-2{,}861.06\ \mathrm{US\$\,h^{-1}}$, representing a value of cost per exergy unit difference equal to $-133.35\ \mathrm{US\$\,MW^{-1}\,h^{-1}}$. Thus, using an absorption chiller, it is possible to increase the annual cost flow rate difference in US$ 75,609.01 per fermentation vat, representing a payback period of 1.59 years (considering five fermentation vats).

4 CONCLUSIONS

The investigation of a cooling system for the ethanol fermentation process using an absorption chiller and a cooling tower has been described in this paper. A dynamic model for the fed-batch fermentation process coupled with a quasi-steady state model for the absorption system was developed under industrial conditions.

The simulation with the new configuration of the refrigeration system (absorption chiller and cooling tower) showed that it is possible to reduce the fermentation temperature by around $1\ ^{\circ}\mathrm{C}$ and increase the fermentation efficiency by around $0.8\ \%$, representing an annual ethanol increase of around $240\ \mathrm{m^3}$ per fermentation vat. These results can be improved by decreasing the temperature to an ideal value for both fermentation kinetics and cell viability. To improve these results, a refrigeration machine with a higher cooling capacity should be used, under controlled operating conditions. An increase in the ethanol concentration of the wine can reduce significantly the energy consumption in the downstream processes, such as the distillation and vinasse concentration. The industrial losses, especially those related to contamination, can be minimized with a decrease in or maintenance of temperature.

The thermoeconomic analysis shows that it is possible to increase the annual cost flow rate difference in US$ 75,609.01 per fermentation vat using the absorption chiller and cooling tower configuration to refrigerate the fermentation process, representing a payback period of 1.59 years.

The results of this study demonstrated the potential application of the absorption chiller for refrigeration in the fermentation process. Absorption refrigeration powered by industrial waste heat is an excellent energy saving option in a co-generation system in sugar and ethanol plant. This may also promote an increase in the energy balance of the ethanol production process, whose current value is around 8.5. All of these advantages contribute also to the competitiveness and sustainability of ethanol.

ACKNOWLEDGEMENTS

The authors would like to acknowledge Usina Cerradinho Açúcar e Álcool S/A for making available the process data and the FINEP/PROABS project for the financial support of this study.

REFERENCES

Albers, E., Larsson, C., Lidén, G., Niklasson, C., and Gustafsson, L. (2002). Continuous estimation of product concentration with calorimetry and gas analysis during anaerobic fermentations of *Saccharomyces cerevisiae*. *Thermochimica acta*, 394:185–190.

Aldiguier, A. S., Alfenore, S., Cameleyre, X., Goma, G., Uribelarrea, J. L., Guillouet, S. E., and Molina-Jouve, C. (2004). Synergistic temperature and ethanol effect on *Saccharomyces cerevisiae* dynamic behaviour in ethanol biofuel production. *Bioprocess and Biosytems Engineering*, 26(4):217–222.

ASHRAE (2001). *HVAC Fundamentals Handbook*. American Society of Heating, Refrigerating and Air-Conditioning Engineers.

Atala, D. I. P., Costa, A. C., Maciel, R., and Maugeri, F. (2001). Kinetics of ethanol fermentation with high biomass concentration considering the effect of temperature. *Applied Biochemistry and Biotechnology*, 91-93(1-9):353–365.

Bejan, A. and Kraus, A. D. (2003). *Heat Transfer Handbook*. John Wiley and Sons, Inc.

Bejan, A., Tsatsaronis, G., and Moran, M. (1996). *Thermal Design and Optimization*. John Wiley and Sons, Inc.

Bereche, R. P. (2007). Avaliação de sistemas de refrigeração por absorção H_2O / LiBr e sua possibilidade de inserção no setor terciário utilizando gás natural. Master's thesis, Universidade Estadual de Campinas.

Camargo, C. A., Ushima, A. H., Ribeiro, A. M. M., Souza, M. E. P., and Santos, N. F. (1990). *Conservação de Energia na Indústria do Açúcar e do Álcool*. IPT - Instituto de Pesquisas Tecnológicas.

Ghose, T. K. and Tyagi, R. D. (1979). Rapid ethanol fermentation of cellulose hydrolysate. I. Batch versus continuous systems. *Biotechnology and Bioengineering*, 21:1387–1400.

Herold, K. E., Radermacher, R., and Klein, S. A. (1996). *Absorption Chillers and Heat Pumps*. CRC Press.

IAPWS (1995). *Formulation for the Thermodynamic Properties of Ordinary Water Substance for General and Scientific Use*. The International Association for the Properties of Water and Steam.

Jarzebski, A. B. and Malinowski, J. J. (1989). Modeling of ethanol fermentation at high yeast concentrations. *Biotechnology and Bioengineering*, 34:1225–1230.

Klein, S. A. and Alvarado, F. L. (2008). *Engineering Equation Solver*, volume 8.160-3D. F-Chart Software.

Lazzaretto, A. and Tsatsaronis, G. (2006). SPECO: A systematic and general methodology for calculating efficiencies and costs in thermal systems. *Energy*, 31:1257–1289.

Lee, J. M., Pollard, J. F., and Coulman, G. A. (1983). Ethanol fermentation with cell recycling: computer simulation. *Biotechnology and Bioengineering*, 25:497–511.

Misra, R. D., Sahoo, P. K., Sahoo, S., and Gupta, A. (2003). Thermoeconomic optimization of a single effect water/LiBr vapour absorption refrigeration system. *International Journal of Refrigeration*, 26:158–169.

Patterson, M. R. and Perez-Blanco, H. (1988). Numerical fits of the properties of lithium-bromide water solutions. *ASHRAE Transactions*, 94(2):2059–2077.

Phisalaphong, M., Srirattana, N., and Tanthapanichakoon, W. (2006). Mathematical modeling to investigate temperature effect on kinetic parameters of ethanol fermentation. *Biochemical Engineering Journal*, 28:36–43.

Rao, J., Das, M., and Das, S. K. (2009). Changes in physical and thermo-physical properties of sugarcane, palmyra-palm and date-palm juices at different concentration of sugar. *Journal of Food Engineering*, 90:559–566.

Szargut, J., Morris, D. R., and Stewart, F. R. (1988). *Exergy analysis of thermal, chemical and metallurgical process*. Hemisphere Publishing Corporation.

Torija, M. J., Rozés, N., Poblet, M., Guillamón, J. M., and Mas, A. (2003). Effects of fermentation temperature on the strain population of *Saccharomyces cerevisiae*. *International Journal of Food Microbiology*, 80:47–53.

RESPONSIBILITY NOTICE

The authors are solely responsible for the printed material included in this paper.